Low-temperature dynamic susceptibility of thin $Cd_{1-x}Mn_xTe$ films

Sharat Chandra* and L. K. Malhotra
Thin Film Laboratory, Department of Physics, Indian Institute of Technology, New Delhi 110 016, India

Sandip Dhara* and A. C. Rastogi
Semiconductor Laboratory, Materials Division, National Physical Laboratory, New Delhi 110 012, India

(Received 29 February 1996; revised manuscript received 10 June 1996)

Dynamic susceptibility and electrical resistance of thin films of $Cd_{1-x}Mn_xTe$ ($0 \leqslant X \leqslant 0.6$) deposited on Corning 7059 glass substrates at a 650-K substrate temperature were studied in the 20–300-K temperature range. The existence of an interstitial MnTe phase and a low-temperature spin-glass phase for $X > 0.25$ has been observed. The low-temperature magnetic and resistive properties of the thin films have been correlated, which provide some different insights in the exchange mechanisms taking place in these materials. [S0163-1829(96)01143-5]

I. INTRODUCTION

The dilute magnetic semiconductor (DMS) encompasses any semiconductor with a fraction of its constituent ions replaced substitutionally by ions bearing a net magnetic moment. The DMS family includes the II-VI, III-V, and IV-VI compounds alloyed with the transition-metal ions, e.g., Mn^{2+}, Fe^{2+}, Co^{2+}, etc. DMS with Mn^{2+} ions substituted in various II-VI hosts[1–5] have been the most extensively studied as the solubility of Mn in II-VI hosts is maximum. The DMS are of interest for their magnetic[6–9] and magneto-optical[10–14] properties such as spin-glass transition, giant Faraday rotation, etc. In $Cd_{1-x}Mn_xTe$ (CMT), for example, these magnetic features begin to show enhanced effects with variation in Mn concentration. The interaction between localized magnetic moments of Mn^{2+} and the conduction and/or valence-band electrons results in these unique effects. These exchange interactions are essentially of two types: the strong Kondo-like sp-d exchange between spins of band electrons and localized magnetic moments, affects the optical properties, while the weaker Heisenberg interion exchange (d-d exchange) affects the magnetic properties. The behavior of DMS alloys in a magnetic field is like that of the nonmagnetic semiconductors, except that the g factor is modified by the sp-d exchange interaction.[15–17] The splitting between the $\uparrow$ and $\downarrow$ spin states depends on the magnetization and hence on the temperature, composition, and magnetic field. The d-d exchange in DMS alloys has been calculated perturbatively by Larson,[16] who showed that it has contributions from three classes of interactions. The two hole processes, namely, the hybridization-induced superexchange between the Mn $3d$ and Te $5p$ states dominate.[16] One-electron and one-hole processes, known as the Bloembergen-Rowland (BR) mechanism, have about 5% contribution and two-electron processes, viz., the Rudderman-Kittel-Kasuya-Yosida (RKKY) interaction, are negligible.[18] In the wide gap DMS alloys, the d-d interaction is primarily a nearest-neighbor interaction. For instance, in CMT, the next-nearest-neighbor exchange integral $J2$ is typically about five to ten times smaller than the nearest-neighbor exchange integral J_1 ($J2/J_1 \approx 0.1$).[18] In a tetrahedral environment, the atomic ground state of $Mn^{2+}(3d^5)$ is ${}^6S_{5/2}$ with a negligibly small crystal-field splitting, and hence it can be viewed as an orbital singlet with $S = \frac{5}{2}$.

The nature and extent of these magnetic interactions can be probed by studying the low-field susceptibility in the DMS system in which Mn concentration (X) is varied. In general, for $X \geqslant 0.005$, DMS's are paramagnetic,[1] show a magnetic phase transition[18,19] as defined by a cusp at a critical temperature T_g for $X \geqslant 0.02$, and form an antiferromagnetic phase for $X > 0.60$.[19] So, the X-T_g plot maps out a magnetic phase diagram,[20] with the low-temperature phase representing a spin glass.[21] In the paramagnetic region, the magnetic susceptibility, χ, follows Curie's law.[19] The Curie-Weiss temperature $\Theta(X)$ obtained is negative, indicating antiferromagnetic interactions between the spins.[22,23] At temperatures below T_g, the magnetic moments are randomly disordered and display many of the characteristics of a spin-glass phase, such as the specific heat which has a linear temperature dependence and does not show any anomaly at T_g.[24] Typically, in a DMS below T_g, different magnetic phases (paramagnetic and spin-glass phases and antiferromagnetic clusters) coexist in the sample.[25] The number of different atoms in different states is a function of X. For example, for $X = 0.65$ in CMT, neutron-diffraction studies show the absence of the long-range order[25] and only 50% of the magnetic atoms are ordered in clusters with antiferromagnetic ordering of the third type. The electron-paramagnetic-resonance (EPR) measurements show a slowing down of the spin fluctuations as T_g is approached from above.[26] The spin-glass behavior is thus attributed to the combined effects of the frustration of the antiferromagnetic interaction on an fcc/hcp lattice and the randomness due to dilution.[27] The ground-state properties of the frustrated quantum Heisenberg antiferromagnets on a cubic lattice have been investigated theoretically for clusters containing 4–36 atoms.[28] It has been found that for $0.00 \leqslant (J_2/J_1) \leqslant 0.34$, the dominant magnetic ordering is of short-range type. The optical and electrical properties of two-dimensional DMS systems are very sensitive to the magnetization[18,29] and hence can be studied by the conventional techniques.[29] In all the cases, suppression of antiferromagnetic order is observed on

the short-range cluster scale.[28] It can be said that thermodynamically, in the limit of low dimensionality and in the absence of spatially anisotropic magnetic interactions within the plane containing the spins, magnetic ordering is not possible because of the finite-size effects, which become more important than the magnetic ordering effects.[25,28]

It is clear that low-temperature behavior of the DMS alloys depends on the detailed topology of the Mn sublattice. A change in nearest-neighbor environment of Mn ions alters the nature of the short-range magnetic ordering.[19] We have investigated exchange interaction dynamics in thin CMT films deposited by closed space sublimation both in the dilute and higher Mn concentration range using low-field dynamic susceptibility as a diagnostic tool in conjunction with electrical resistivity measurements. The occurrence of spin-glass phase, deviation from the Curie-Weiss law, and importance of the MnTe interstitial sublattice (different from bulk) have been revealed from these studies. This paper presents these results.

II. EXPERIMENTAL DETAILS

The $Cd_{1-x}Mn_xTe$ films were deposited on to Corning 7059 glass substrates, maintained at 350 °C, by sublimation from different stoichiometric alloys (with X values from 0.01 to 1.0), and prepared by melt quenching. Details of film deposition and compositional characterization have been reported in an earlier publication.[30] The studied compositions correspond to nearly $X=1.00$, 0.60, 0.50, 0.40, 0.30, 0.25, 0.20 (± 0.01) in the higher Mn concentration range and $X=0.10$, 0.06, 0.04, 0.02, 0.00 (± 0.01) in the dilute range. The low-temperature ac susceptibility of the films was measured in the 300–20-K temperature range using a Sumitomo SRD-204 cryostat with facility for simultaneous measurement on eight samples. A double secondary coil arrangement with one coil wound opposite to the other was used as pick-up coil to increase the signal-to-noise ratio. The primary coil was excited by an amplified ac signal from a signal generator to produce a harmonic excitation magnetic field. The real and imaginary components of the induced signal were measured by a lock-in amplifier interfaced with an IBM PC. The susceptibility measurements were done on samples both in the zero-field cooling (ZFC) and field cooling (FC) modes[31] in the presence of an external static magnetic field. The magnitude of the static external field was always greater than that of the dynamic excitation field. To make the data representative of the magnetization in the films and for proper comparison between the films of different X values, the data were normalized with respect to the sample volume and the area under the curve (found by integrating the susceptibility values over the entire temperature range divided by the calculated area). The resistivity of the films was measured in the 300–20-K temperature range using a standard four probe technique in the same cryostat. For the resistivity measurements, four silver pads 250 μm apart were deposited on the film surface and contacts were taken from them.

III. RESULTS AND DISCUSSION

The divalent Mn atoms have a $3d^5 4s^2$ configuration. After contributing the two $4s$ electrons to the lattice, Mn^{2+} ions have a $3d^5$ configuration and a $^6S_{5/2}$ ground state.[32] A spherically symmetric S state cannot be affected by a crystalline electric field. However, it is known that a crystal-field splitting of the ground state of Mn^{2+} does occur.[32] This is because it is not a pure ^6S state but consists of an admixture of higher-lying levels.[32] The effects of these admixtures are relatively small and have been neglected here as we are concerned only with the gross electronic properties like the magnetic susceptibility and resistivity.

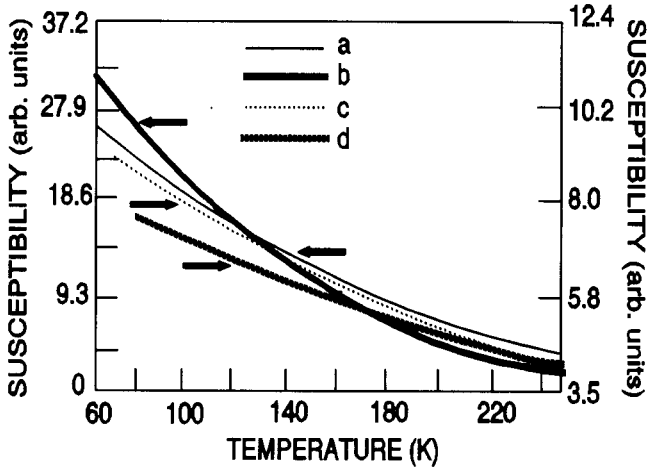

FIG. 1. Real susceptibility versus temperature plot for $X=0.25$ films deposited on Corning 7059 glass and Si(111) substrates. (a) and (b) Films on Si(111) and Corning 7059 glass at 313 Hz; (c) and (d) films on Si(111) and Corning at 1-KHz measuring frequency, respectively.

The ac susceptibility of the $Cd_{1-x}Mn_xTe$ films deposited on Corning 7059 glass and Si(111) substrates were measured in the temperature range 300–20 K at 73-Hz, 313-Hz, and 1-KHz signal frequencies. All samples show paramagnetic behavior at higher temperatures (>50 K) and the magnitude of susceptibility was maximum at 73 Hz and decreased with increasing frequency. Figure 1 shows the variation of susceptibility with temperature at 313-Hz and 1-KHz signal frequencies for a typical film of composition $X=0.25$, deposited on Corning 7059 and Si(111) substrates, in the high-temperature (300 to 60 K) range. Susceptibility of the film on Corning 7059 substrate was smaller in magnitude. This is attributed to smaller grain size of the $Cd_{0.75}Mn_{0.25}Te$ film on Corning than on Si(111).[30]

The real (χ') and imaginary (χ'') parts of the FC normalized susceptibility data for the Corning 7059 glass substrate are shown in Fig. 2 both for the cooling and the heating cycle in the temperature range 300–20 K. It is clear that Corning glass is diamagnetic in the entire temperature range. The magnitude of χ'' increases with a decrease in temperature until it saturates in the low-temperature range. The negative value of χ'' at temperatures >250 K is an artifact of the lock-in amplifier phase setting being >90°. Figures 3 and 4 show the real and imaginary parts of FC normalized susceptibility variation over the 300–20-K temperature range for a $Cd_{1-x}Mn_xTe$ film on Corning substrate in the dilute regime ($X=0.02$), both for the cooling and the heating cycle. It shows a paramagnetic behavior without any magnetic phase transformation since no abrupt changes in χ'' values are ob-

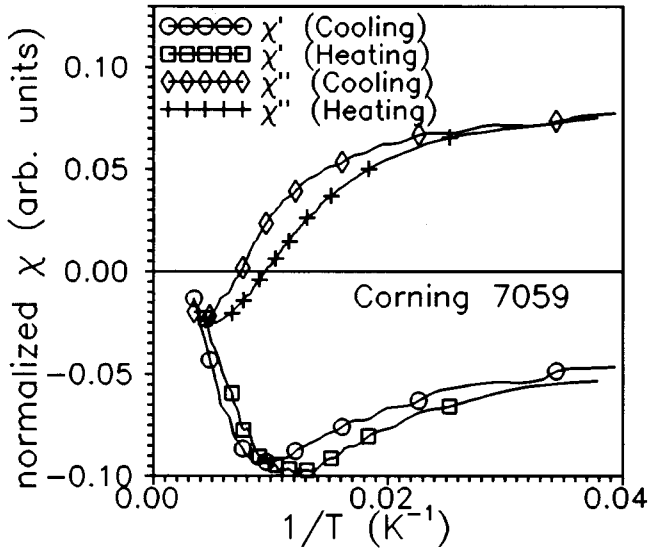

FIG. 2. Low-temperature susceptibility of Corning 7059 glass for the cooling and heating cycles. The data show thermal hysterisis.

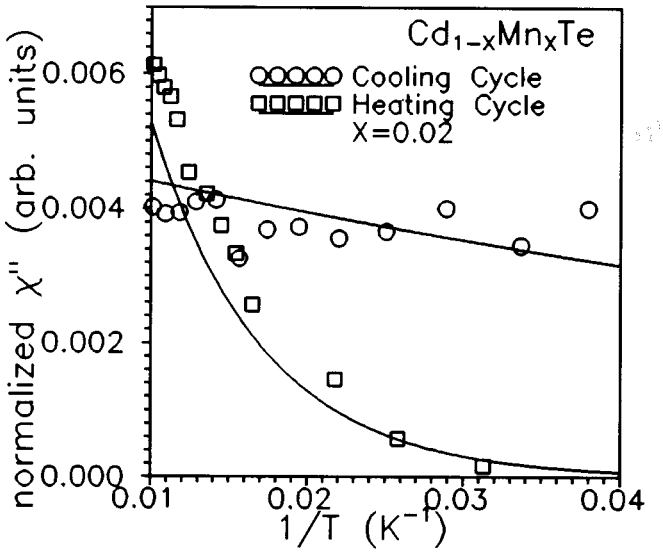

FIG. 4. Imaginary susceptibility versus temperature plot of $X=0.02$ films deposited on Corning 7059 glass at a 650-K substrate temperature.

served (Fig. 4). The thermal hysterisis effects are also observed in the real and imaginary parts of the susceptibility in both the cycles. In contrast, for the CMT films having a higher Mn concentration range, the zero-field cooled samples exhibit a broad hump in the χ' values at low temperatures ($\leqslant$40 K) and the χ'' data also display a cusp at temperatures somewhat higher than that for the χ'. The occurrence of the broad hump instead of a sharp maxima in the χ' is explained on the basis of the interactions of the magnetic sublattice with phonons, which increase the effective relaxation time of the magnetic spins. Figures 5 and 6 show the χ' and χ'' data for the ZFC and FC cases during the heating cycle for typical films with $X=0.4$ and 0.6, respectively. An occurrence of a magnetic phase transition, typically the formation of a low-temperature spin-glass phase in higher-X samples, is indicated. The different spin-glass transition temperatures observed in the higher-X films are given in Table I. Information about the first-neighbor interaction can be obtained from the spin-glass transition by application of a suitable model. We have applied the scaling model[23] to such a transition assuming that for a continuous random distribution, $XR_{ij}^{3}=$const, where R_{ij} denotes the typical distance between the magnetic ions i and j at concentration X. Using this expression, with a known functional form for the radial dependence of the ex-

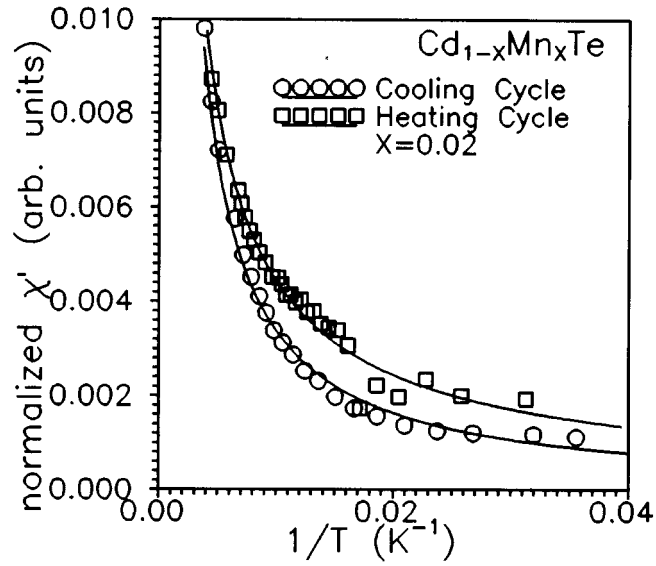

FIG. 3. Real susceptibility versus temperature plot of $X=0.02$ films deposited on Corning 7059 glass at a 650-K substrate temperature.

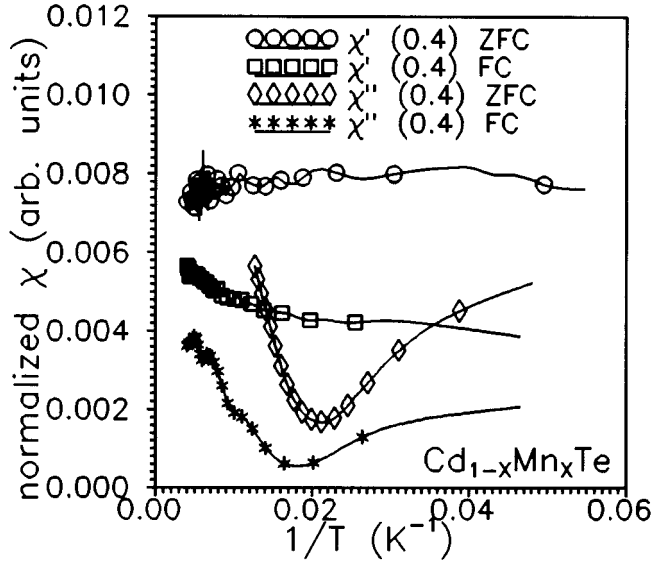

FIG. 5. Normalized susceptibility plots for $X=0.4$ films deposited on Corning 7059 glass at a 650-K substrate temperature for both the field cooled and zero-field-cooled cases.

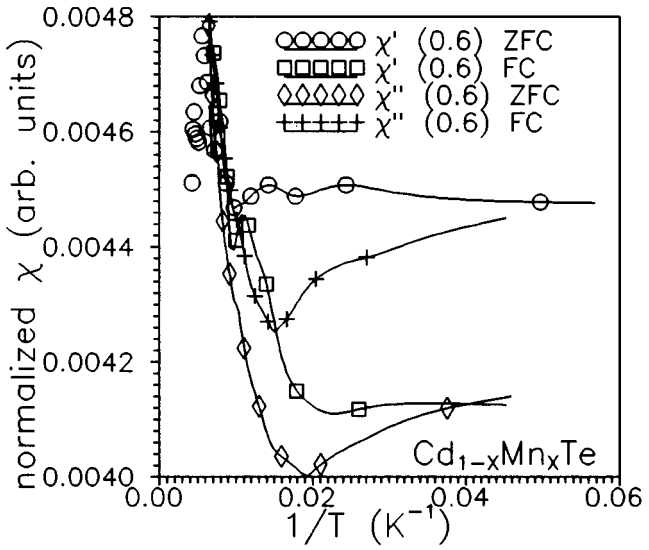

FIG. 6. Low-temperature susceptibility plots for $X=0.6$ films deposited at 650 K on Corning 7059 glass for both the FC and ZFC cases.

change interaction, we get a theoretical prediction that can be compared with the observed experimental data. The functional form used by us can be represented empirically in a simplified manner as[23]

$$k_B T_g \approx A J_1(R) S(S+1), \tag{1}$$

where A is an arbitrary constant ($A<0.5$ for our case) dependent on the decay of the nearest-neighbor exchange. Details of the exact procedure for a continuous as well as discrete distribution of magnetic ions can be found elsewhere.[23] It may be pointed out that the above equation is based on the assumption that T_g is related to the interaction energy at an average distance (R) between the magnetic ions and only the first-neighbor exchange interactions dominate. The first-neighbor exchange integral values thus obtained are also given in Table I. Both the transition temperature and the corresponding exchange integral have higher magnitude than those reported for single crystals of $Cd_{1-x}Mn_xTe$.[1] We also observe that the magnitude of the first-neighbor Mn-Mn exchange integral (J_1) increases with increasing X values. The spin-glass transition is observed in only the ZFC susceptibility data, whereas the FC susceptibility data show no maxima in the χ' values, indicating that the spin-glass phase formation does not occur. This behavior can be understood in terms of orientation of magnetic spins, as explained in the next section. Figures 7 and 8 show ZFC and FC susceptibility data for films of CdTe ($X=0.0$) and MnTe ($X=1.0$), respectively. It is inferred that the CdTe films are diamagnetic in nature, while the MnTe films are paramagnetic at higher temperatures and show a spin-glass phase at $\approx$50 K. Correspondingly, the χ'' variation with temperature for MnTe films shows a cusp at a temperature somewhat higher than that of the maxima in the χ' data. The spin-glass phase as observed in pure MnTe films significantly modifies the temperature-dependent magnetic susceptibility behavior of MnTe and CdTe alloyed $Cd_{1-x}Mn_xTe$ thin films.

TABLE I. The spin-glass temperatures and first-neighbor exchange integral values observed for different composition films.

% Mn (X)	T_{sg} (K)	J_1/k_B (K)
0.4	25.12	−10.71
0.5	32.96	−11.31
0.6	40.98	−11.71
1.0	49.54	−8.49

Temperature-dependent resistivity variation for the $Cd_{1-x}Mn_xTe$ films with various X values was also studied. In the dilute regime, $Cd_{1-x}Mn_xTe$ films have a high resistivity (of the order of 10-MΩ-m), while the resistivity of films

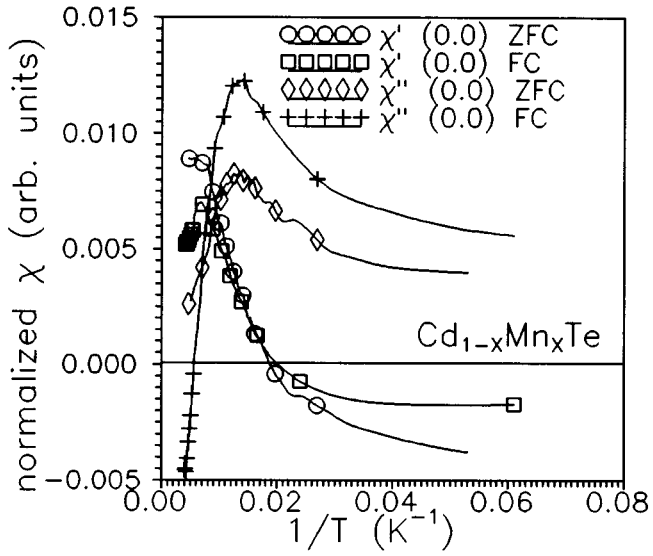

FIG. 7. Normalized susceptibility plots for the pure CdTe ($X=0.0$) films deposited at 650 K for both the FC and ZFC cases.

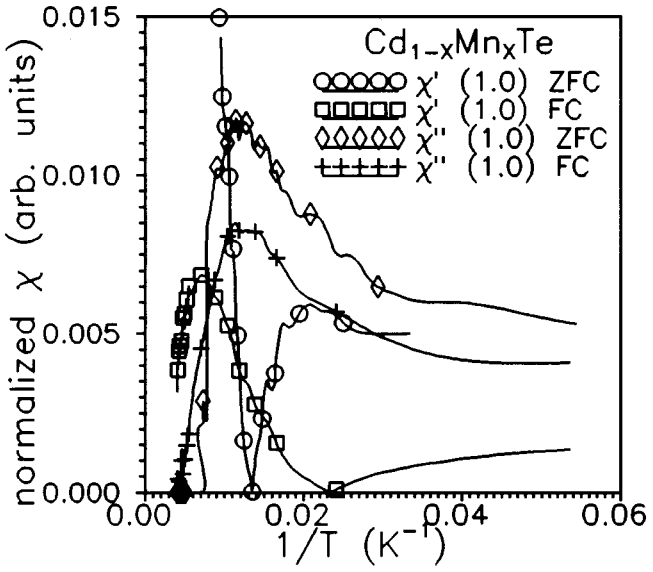

FIG. 8. Low-temperature normalized susceptibility plots for pure MnTe ($X=1.0$) deposited at 650 K for both the FC and ZFC cases.

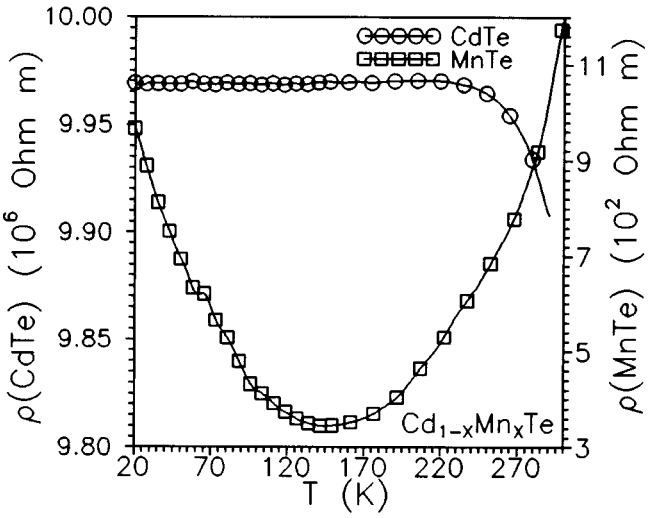

FIG. 9. Low-temperature resistivity plots for CdTe and MnTe films deposited at 650 K on Corning 7059 glass.

with higher Mn concentration ($X \geqslant 0.25$) decreases to typically 0.5-MΩ-m with increasing X. Figure 9 shows the characteristic dependence of the low-temperature resistivity for pure CdTe and MnTe films. The resistivity of CdTe films increases initially with a decrease in temperature and saturates to a constant value below 250 K, a behavior typical of a high-resistivity semiconductor. The MnTe films, on the other hand, exhibit a broad minima at 130 K. Below 130 K, the behavior of the film is semiconductorlike, and above it the film behaves like a metallic film. This semiconductor-to-metal-like transition has genesis in the magnetic properties of the material. Figure 10 shows the normalized resistivity versus temperature plot for the films with X in dilute range, i.e., for $X=0.00$, 0.02, 0.04, and 0.06. The data have been normalized with respect to the film surface area and the area

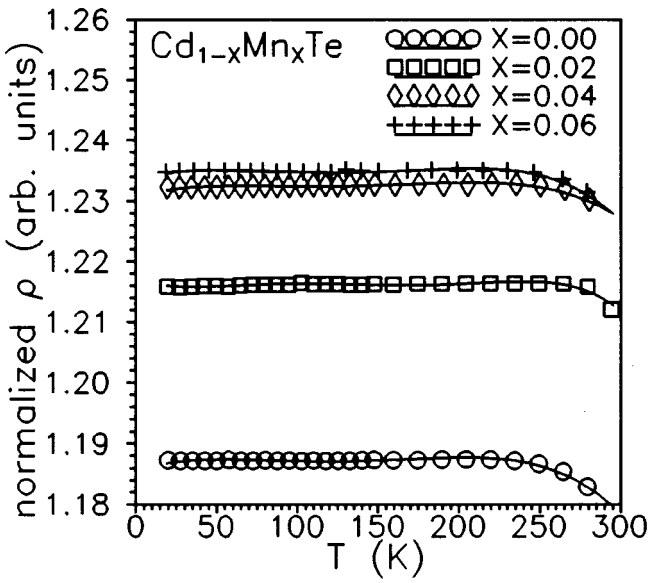

FIG. 10. Typical low-temperature normalized resistivity plots for $Cd_{1-x}Mn_xTe$ thin films in dilute range ($X<0.1$).

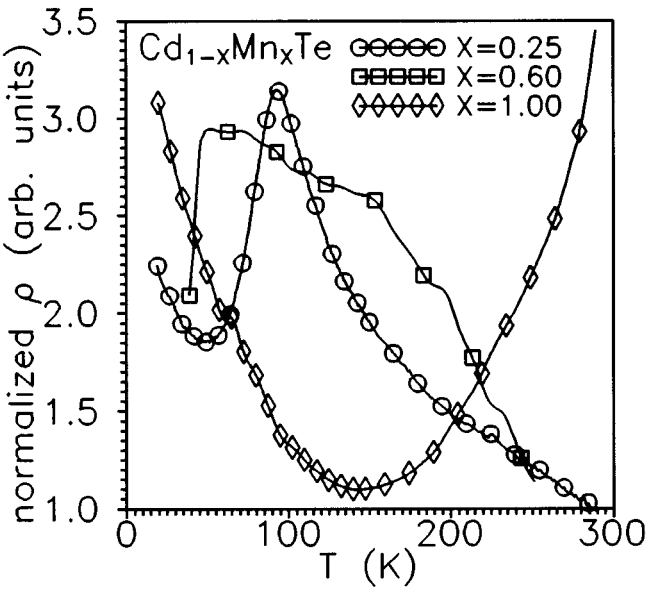

FIG. 11. Typical normalized resistivity versus temperature plots for $Cd_{1-x}Mn_xTe$ thin films in alloy range ($0.1<X<1.0$).

under the curve to present the data on comparable scales. We see that the resistivity behavior of the films having low-X values is similar to that of the CdTe. The resistivity is constant from 20 to 250 K and decreases thereafter. In the dilute range, the CdTe films have the least resistivity which increases with increase in Mn concentration. The normalized resistivity of the higher-X films is shown in Fig. 11 for typical films having $X=0.25$, 0.60, and 1.00. All the films exhibit a resistivity transition from a semiconductorlike to metallike behavior. These transitions temperatures are significantly higher than the spin-glass transition temperatures. We expect that the interaction of electron spins and the Mn magnetic moments is responsible for it, as discussed below. An estimate of the defect densities, which contribute to the two-electron interaction via the electron-phonon meditated exchange, made from the resistivity and optical-absorption data[30] gives the density to be approximately $10^{20}/cm^3$ for all the higher-X films. Due to the high defect density observed, the RKKY-like scattering interactions become as important as the BR mechanism which dominates at low defect densities in these films. Hence, the contribution of the RKKY interactions should also be taken into account in addition to the superexchange phenomenon and BR mechanism.

A. Effect of Mn on magnetic susceptibility

It is evident from the experimental results that $Cd_{1-x}Mn_xTe$ films exhibit susceptibility and resistivity behavior which directly depends on the Mn concentration regime. In the dilute range, behavior is akin to CdTe as the Mn ions behave like Cd ions because they are isolated magnetically. The effect of the magnetic moment and its interaction with the electron spins becomes pronounced for higher Mn concentration films ($X \geqslant 0.25$) and different effects like spin glass and semiconductor to metal-like resistivity transition begin to manifest. An interesting observation is that the spin-

glass transition temperature is higher in the films than that in the single crystals. Clearly, the exchange interactions due to Mn dominate in the films. The thermal hysterisis observed in the films (Fig. 3) is understood on the basis of the time dependence of the relaxation time. The relaxation time is the temperature-dependent time in which the spins interact with the applied field which is modified by the kinetic interactions taking place between the magnetic ions. Since the rate of cooling in the experiments is different from the rate of heating, the relaxation time for the above interaction will be different during the cooling and the heating cycles, thus giving rise to the thermal hysterisis as observed in the films. The nonobservation of the spin-glass phase in the FC susceptibility can be explained on the basis of the behavior of magnetic spins in the presence of an external static magnetic field. The magnetic spins are bound by the external static magnetic field and thus are not able to respond to the dynamic excitation field. Hence, the behavior of the susceptibility in the field cooled mode is paramagnetic.

It is known that the dilute magnetic compounds exhibit the antiferromagnetic III (AFM III) ordering of the magnetic ions.[32] In the $Cd_{1-x}Mn_xTe$, the formation of the spin glass at low temperatures is a consequence of the frustrated antiferromagnetic arrangement of the Mn ions, which leads to a freezing of the spins in random directions under the influence of a magnetic field as the transition temperature is reached.[33] This freezing of spins corresponds to a cusp in the real part of the susceptibility value for the film, while the imaginary part shows a maxima in the vicinity of the transition temperature. The real part of the susceptibility at temperatures >100 K follows a Curie-Weiss law, $\chi'=C/[T-\Theta(X)]$, C being the Curie constant and $\Theta(X)$ the Curie temperature. When the temperature is lowered below 100 K, deviations from the linear behavior predicted by the Curie law start appearing in the χ' behavior. This has been reported both in the metallic and insulating spin glasses,[33–35] indicating that on a local scale, strong magnetic correlations start developing far above the freezing temperatures.[34–36] The freezing temperature of a spin glass has been shown to have a frequency dependence. As the measuring signal frequency is increased, the transition temperature increases.[36] The frequency dependence of susceptibility indicates that the establishment of full thermal equilibrium between the magnetic spins in the films is a dynamic process affected by the local relaxation times. Superexchange in these materials is an indirect interaction meditated by the anions. For II-VI DMS's with a zinc-blende structure, the Mn-Mn second-, third-, and fourth-neighbor exchange are all meditated by two anions and one cation[36] (sp-d exchange). The competitive process of the scattering of charge carriers at the spin centers in presence of a magnetic field leads to an indirect exchange interaction meditated through phonons, which is RKKY-like in nature and which oscillates strongly with distance R between the two spins. This phonon meditated exchange results in the observation of the large transition width, as phonons increase the relaxation time of the freezing process and do not allow the magnetic spins to freeze on approaching T_g. The exchange interaction integral $J_1(R)$ is written as

$$J_1(R)=J_0\,\frac{\cos(2k_FR+\varphi_0)}{(k_FR)^3},\quad R\to\infty. \tag{2}$$

Here, J_0 and φ_0 are constants and k_F is the Fermi wave number of the host lattice, CdTe in our case. Thus, there are two competiting phenomena taking place within the material: freezing of the spins and interaction of magnetic moments with the phonons. Since the distances between the spins are random, some of the interactions favor a parallel alignment and others favor an antiparallel alignment. Thus no single favorable alignment can be found, thereby freezing the magnetic moments in random directions on approaching T_g.[37] The phonons, on the other hand, prevent this freezing, leading to the absence of a sharp transition. The real situation is much more complex than this simple picture, and involves in addition, the nearest-neighbor interactions between the magnetic spins. When we take into account these interactions, Curie-Weiss temperature can be written empirically as

$$\theta(X)=\frac{2S(S+1)}{3k_B}\sum_R J_1(R)P_X(R). \tag{3}$$

Here, $P_X(R)$ is the probability that an atom possesses magnetic moment, which is just the X value, k_B—the Boltzmann constant, S—the spin quantum number ($=\frac{5}{2}$ for Mn), and X—the concentration of magnetic atoms. It is assumed that the magnetic moment of the atom is independent of concentration and temperature. Equation (3) is qualitatively similar to Eq. (1) above. This is because the magnetic subsystem in a DMS consists of a random array of magnetic ions statistically distributed over the cation lattice sites and coupled to nearest and next-nearest neighbors by exchange interactions. The Curie-Weiss temperature probes the sum of all interactions, which, in our case, is antiferromagnetic. The low-temperature spin-glass transition probes the long-ranged tail of the interaction, which also depends on the effective magnetic coupling of the magnetic ions and decays as R^{-n}, where n is a fitting parameter.[22,33] For materials where the spatial decay of exchange is fast ($n>6$ and $J_2/J_1<0.3$), the only dominant interactions are the nearest-neighbor type and the two entities qualitatively describe the same interactions.[33]

The calculated values of nearest-neighbor exchange integral, J_1, are significantly higher in magnitude than those reported for single crystals of CMT in literature[1] which suggests stronger Mn interaction in higher-X $Cd_{1-x}Mn_xTe$ films. Mn ions occupy the substitutional as well as interstitial sites in the CdTe lattice at higher Mn concentrations.[30] At the substitutional site Mn forms the $Cd_{1-x}Mn_xTe$ lattice, whereas the interstitial Mn interacts with the neighboring Te ions and forms an interstitial MnTe sublattice, having properties very similar to that of pure MnTe. The average magnetic properties of the $Cd_{1-x}Mn_xTe$ films should thus be determined by taking into account the contributions from this sublattice also. We observe that our MnTe films have a higher spin-glass transition temperature of 49.5 K as compared to $\approx$42 K in the bulk. Recently, MnTe has been grown by molecular-beam epitaxy in the zinc-blende phase which has a transition temperature of $\approx$60 K and $J_1/k_B\approx-12.3$ K.[38] A high spin-glass transition temperature for the MnTe films by implication should enhance the transition temperatures for $Cd_{1-x}Mn_xTe$ films as well, if the MnTe sublattice contribution to the overall magnetic properties are significant. With an increase in Mn ion concentration in the films, a corresponding increase in the first-neighbor exchange mag-

nitude will imply that more Mn ions are occupying the interstitial sites, resulting in increased Mn ion activity in the CdTe sublattice. If the Mn ions were to occupy only the substitutional sites, the number of magnetic neighbors of a magnetic ion would remain the same as the distribution of Mn in CdTe sublattice is generally random. Consequently, the magnitude of the exchange integral would not be much effected.

The formation of the interstitial MnTe sublattice likewise effects the low-temperature electrical resistivity of the $Cd_{1-x}Mn_xTe$ films. When an external magnetic field is applied at temperatures close to the spin-glass transition temperature, the magnetic-field-induced tendency to align along the magnetic-field direction is countered by the lowering temperature-induced spin-glass random freezing. This coupled with the fact that the susceptibility magnitude depends strongly on the time constant of the relaxation process of the magnetic sublattice makes the observed susceptibility values dependent on the input signal frequency.[33] The spin-relaxation times have been found to increase to a very large magnitude as the spin-glass transition temperature is approached.[39] A large magnitude of the relaxation times, which leads to the freezing of the spins in the magnetic sublattice, indicates that the spin-glass phase is in a nonequilibrium state in the thermodynamic sense.[39] An insight into the dynamics of a spin-glass transition can be obtained by measuring the real and imaginary parts (χ' and χ'') of the complex susceptibility $\chi(\omega)$.[40,41] If the magnetization relaxes with a single relaxation time, τ, χ', and χ'' can be expressed for the input signal frequency ω, as[33]

$$\chi'(\omega)=\chi_S+\frac{\chi_T-\chi_S}{1+\omega^2\tau^2} \tag{4}$$

and

$$\chi''(\omega)=\omega\tau\frac{\chi_T-\chi_S}{1+\omega^2\tau^2}, \tag{5}$$

where χ_T is static isothermal susceptibility and χ_S the static adiabatic susceptibility. The plot of χ' versus χ'' with ω as a parameter, known as the Cole-Cole plot, yields a semicircle.[33] On the other hand, if the relaxation of the magnetization process is governed by a distribution of relaxation times rather than a single one, these plots are described by arcs rather than semicircles.[33] The plots for the films of typical composition $X=0.00$, 0.06, 0.50, 1.00, and Corning 7059 glass are shown in Fig. 12. We observe that the plot for the CdTe ($X=0.00$) and MnTe ($X=1.0$) films describes a semicircle, indicating that the relaxation process in both the CdTe and MnTe is governed by a very small bandwidth of relaxation time. As the Mn concentration in CdTe films is increased to form the $Cd_{1-x}Mn_xTe$, the semicircle turns into arc of semicircle indicating that the magnetic relaxation is characterized by a broad bandwidth of times. The physical origin of the distributed magnetic relaxation is attributed to scattering processes at the magnetic moment sites in the semiconducting lattice.

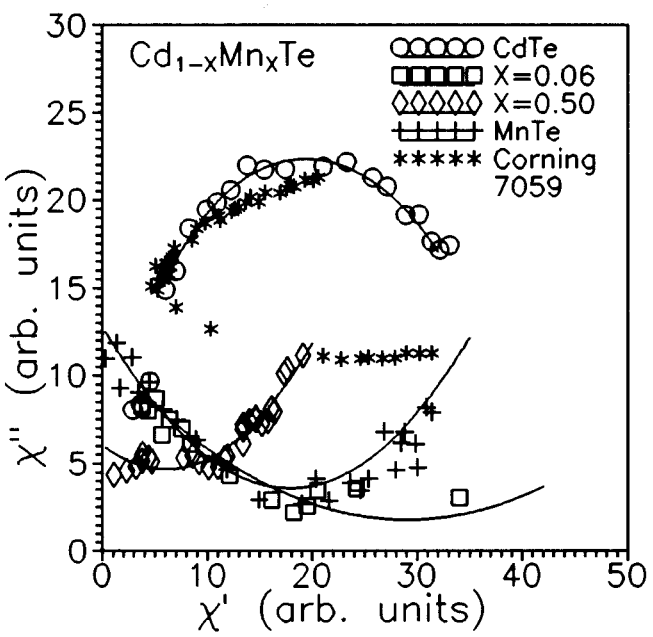

FIG. 12. Real versus imaginary susceptibility (Cole-Cole plots) for some typical films of $Cd_{1-x}Mn_xTe$.

B. Low-temperature resistive properties

Since the formation of the interstitial magnetic MnTe sublattice influences the electrical resistivity, particularly at low temperatures, this constitutes another way to study the spin-glass phenomena.[42,43] The temperature dependence of the electrical resistivity for CdTe and MnTe thin films are shown in Fig. 9. Figures 10 and 11 show the low-temperature resistivity plots of $Cd_{1-x}Mn_xTe$ films in typical dilute and alloy ranges corresponding to different values of X. The films in the dilute range show constant resistivity values in the 20–250-K temperature range, with a nominal decrease above 250 K, typical of semiconductors. The higher-X films show a contrasting behavior. They exhibit a transition from semiconductorlike behavior at higher temperatures to metal-like behavior below 100 K. In the dilute X films, the resistivity of the films increases as the Mn concentration increases. It implies that Mn incorporation enhances the p-type nature of the as-deposited CdTe films. In the low-X limit, Mn ions substitute the Cd ions in the CdTe lattice, and do not contribute extra charge carriers for conduction processes in the semiconductor. However, as the Mn concentration in the films approaches alloy range ($X>0.20$), the excess Mn ions get incorporated at the interstitial sites in addition to the substitutional ones. The interstitial MnTe sublattice, thus formed, interacts with the $Cd_{1-x}Mn_xTe$ host lattice which results in films with resistivity values much lower in magnitude than the resistivity for pure CdTe. While the low-temperature resistivity of CdTe is of the order of 10-MΩ-m, the resistivity of $X=0.25$ film is of the order of 1-MΩ-m. The $X=0.60$ films have a resistivity of 0.1-MΩ-m and the pure MnTe films have a 1-KΩ-m resistivity at low temperatures. As shown in Fig. 11, initially the resistivity increases roughly linearly as temperature is lowered from 300 K. It shows a broad transition to metal-like resistivity behavior at a temperature which is higher than the spin-glass transition temperature. The semiconductorlike resistivity in the higher-

temperature region follows the T^2 behavior,[44] whereas in the metal-like region, the resistivity is proportional to $T^{3/2}$.[42] These temperature dependencies signify different scattering mechanisms which affect the electron transport in $Cd_{1-x}Mn_xTe$ films at low temperatures. The electron-phonon scattering at the boundaries exhibits $T^{3/2}$ dependence and at the spin sites follows the T^2 dependence.[45] The resistivity at low temperatures has been theoretically linked to the temperature variation of the spin-glass order[46] and to the elementary excitations in the spin glasses.[47–49] The resistivity maximum is a consequence of Kondo-like interactions which take place between the magnetic moments and electrons in the films and thus effect the spin-glass properties.[50–52] To better understand this resistivity behavior in these films, we now examine the temperature dependence of the relaxation time.[47]

In an insulator, at temperatures above the Debye temperature, the relaxation is dominated by the phonon-phonon scattering. The Umklapp process is more important than the normal process. The number of Umklapp events that occur is proportional to the number of short-wavelength phonons present.[47] This implies that the high-temperature resistivity of an insulator is directly proportional to T, as the number of phonons associated with any mode in a material is proportional to T. At temperatures well below the Debye temperature, the phonon-phonon relaxation time shows an exponential dependence on the temperature. As the temperature decreases, the number of Umklapp events decreases very quickly and the phonon-phonon relaxation time increases, just as quickly.[48] Eventually, the phonon-phonon relaxation time becomes much larger than the relaxation time for the defect and grain-boundary scattering and the later mechanisms dominate. Thus the temperature-dependent resistivity follows the relation[48]

$$\rho = \frac{A}{T^3} + \frac{B}{T^2} + CT, \tag{6}$$

where the first term describes the boundary scattering, the second, dislocation scattering, and the third, point defect scattering. Factor A depends on the sample dimensions, B is proportional to the number of dislocations, and C is proportional to the number of point defects.[47,48] For any material at low temperatures, the boundary scattering dominates and the resistivity is proportional to T^3.[48] In a semiconductor, if the electron and hole concentrations are nearly independent of temperature over a wide temperature range, the temperature dependence of the resistivity is determined by the carrier mobilities. However, a different temperature dependence is observed when the relaxation times show a significant energy dependence.[49] A simple model of electron-phonon scattering predicts the resistivities to be proportional to $T^{3/2}$, if the bands are assumed to be parabolic and the Debye approximation is valid.[49] In semiconductors, the occurrence of several equivalent minima in the conduction and several maxima in the valence bands[50] complicates the scattering process as scattering from one minimum to other or from one band to other can occur.[50,51] Further, the bands are not parabolic and optical-phonon scattering at high temperatures can also occur.[52,53] As a result the temperature exponent of the resistivity is proportionally larger than $\frac{3}{2}$. This effect is seen in the T^2 dependence of the resistivity observed in our films.

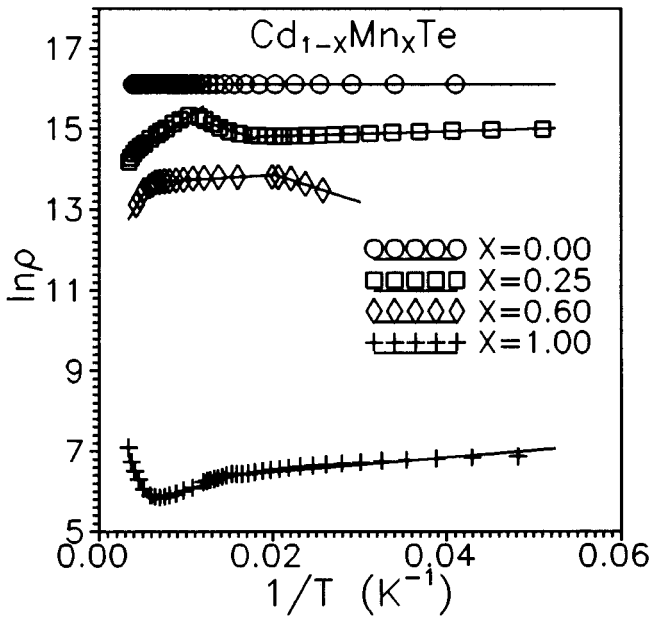

FIG. 13. Plots of $\ln\rho$ versus $\ln(1/T)$ for some typical films used for calculating the activation energy.

The charge-carrier densities observed in the higher-X films are quite high ($n \approx 10^{20}/\text{cm}^3$) (Ref. 30) and remain constant throughout the temperature range studied. The Arrehenious plots for some typical films of CdTe ($X=0.00$), $X=0.25$, 0.60, and MnTe ($X=1.00$) are shown in Fig. 13, in the 300–20-K temperature range. We observe that the CdTe (and the low-X) films show an invariant resistivity behavior in the low-temperature range. Clearly, the $Cd_{1-x}Mn_xTe$ films in the dilute range have a structure similar to that of the CdTe having a homogeneous lattice with Mn at Cd substituted sites. As the Mn concentration increases, the films begin to exhibit three distinct resistivity behaviors at different ranges for the temperatures, e.g., 300–200 K, 200–100 K, and 100–20 K, which are characteristic of the semiconductor- and metal-like behavior. The activation energy for these different regions was calculated by a linear fit of the resistivity data. Figure 14 shows the calculated activation energies for the different regions in films with various compositions with respect to the Mn concentration. We observe that while CdTe has a single positive activation energy throughout the temperature range studied, indicating a semiconducting behavior, all the other films have different activation energies in the different temperature ranges. The activation energies are much smaller than the band-gap energies as determined from the optical measurements. Clearly, low temperatures, the conduction in these films is dominated by the scattering.[53] Excess carriers are generated close to the valence band by magnetic Mn ion dopings in the films. The activation energy dependence at low temperatures is suggestive of the s-d interaction between the s-like conduction-band electrons and d-type transition-metal impurities.[53,54] This interaction is a strongly localized perturbation on the electron gas. On treating the whole effect as an external perturbation, it gives rise to an oscillating term of wave number $2k_F$ (k_F being the moment at the Fermi level),

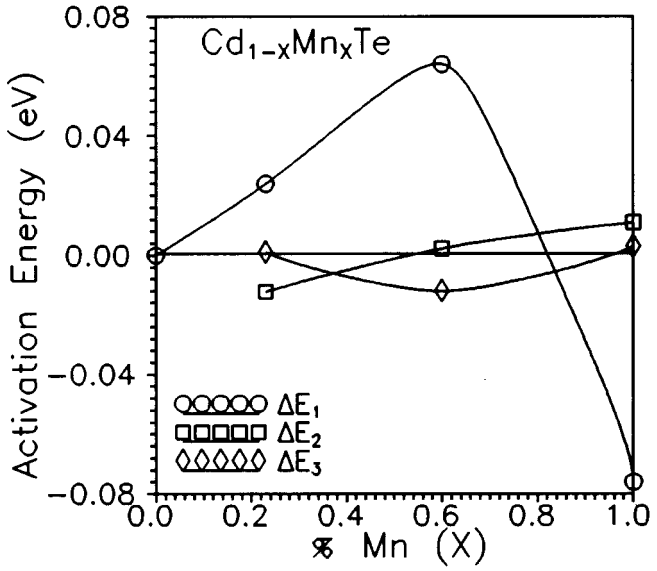

FIG. 14. Activation energies in different temperature ranges as calculated from Fig. 13.

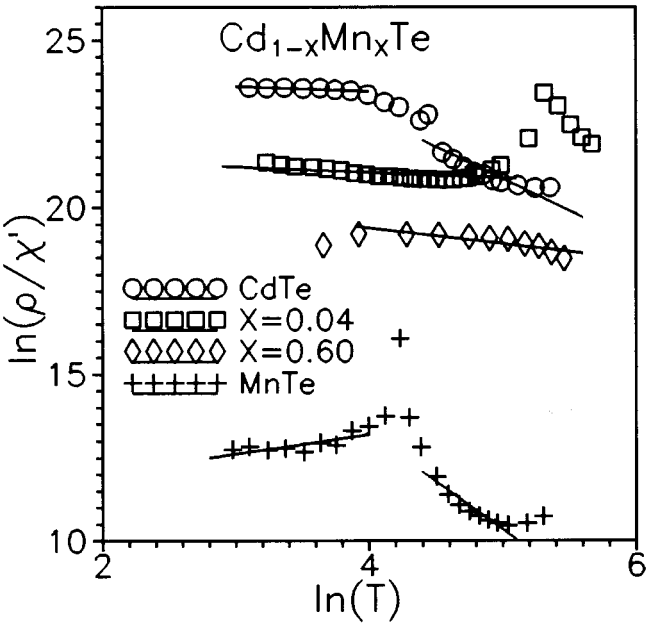

FIG. 15. $\ln(\rho/X')$ versus $\ln(T)$ plots for some typical films. The slope of all the films differs from $\frac{3}{2}$.

falling off as $1/r^3$ at large distances.[54] This is the RKKY interaction which provides a mechanism for the coupling of two adjacent magnetic ion spins.[53] The excess of down-spin s electrons in the vicinity of an up-spin impurity, induces a corresponding up spin on any other impurity spin in its neighborhood. This type of interaction gives rise to complex magnetic and thermal effects in the dilute alloys where the Mn magnetic ions are distributed at random on the solvent CdTe lattice.[54] The spin-dependent s-d interaction is also responsible for the effects observed in the low-temperature electrical resistivity.[53] The nonvanishing residual resistivity at zero K caused by charged impurities is independent of temperature.[53] The probability of scattering from a charged magnetic impurity on integration through a *thermal layer* of k_BT thickness for an energy level $(\varepsilon_F - D)$ below the Fermi level, gives the resistivity as[53]

$$\rho(T) = \rho_0\{1 - 2(J/N)N(\varepsilon_F)\ln(D/kT)\}, \tag{7}$$

where $N(\varepsilon_F)$ is the density of states at the Fermi level, and N is the total number of atoms per unit volume. Since J_1 is essentially negative, this predicts a rapid increase in the residual resistivity as the temperature falls.[53,54] Thus, the resistivity maximum observed in the films is indicative of the antiferromagnetic ordering of the magnetic spins taking place at low temperatures in the alloyed $Cd_{1-x}Mn_xTe$ films.[54] This is also borne out by the density of states calculations,[30] which show a significant increase in the impurity density of states as the Mn concentration is increased in the $Cd_{1-x}Mn_xTe$ films. With increasing Mn concentration the antiferromagnetic ordering temperature also increases, which should result in higher spin-glass transition temperatures, as indeed observed in the films.

The correlation between the low-temperature susceptibility and electrical resistivity of the films has been calculated by s-d exchange model given by Sugihara[55–57] assuming the localization of the d electrons. For an antiferromagnet, the relaxation time τ_{sd} and resistivity ρ_{sd} can be expressed as[56]

$$\tau_{sd} = \frac{2\hbar}{k_BT\omega^{1/2}}\left(\frac{\hbar^2}{2m}\right)^{3/2}\left(\frac{g\mu_B}{J_1/N}\right)\frac{1}{3\chi'(T)}, \tag{8}$$

$$\rho(T) = \frac{3\pi m}{8n\hbar e^2}\left(\frac{2m}{\pi\hbar^2}\right)^{3/2}\left(\frac{J_1/N}{g\mu_B}\right)(k_BT)^{3/2}(3\chi'(T)), \tag{9}$$

where ω is the frequency of measurement of dynamic susceptibility, n the number of charge carriers, and $3\chi'(T) = (2\chi'_\perp + \chi_\parallel)$ is the susceptibility of the film.[57] Thus, from the above two equations, we can write

$$\ln\left[\frac{\rho(T)}{\chi'(T)}\right] = A + \tfrac{3}{2}\ln T, \tag{10}$$

where A is a constant. A plot of $\ln(\rho(T)/\chi'(T))$ versus $\ln(T)$ should thus give a straight line of slope $\frac{3}{2}$. We have plotted Eq. (9) in Fig. 15. We observe a deviation from linearity in the vicinity of spin-glass transition temperature. The peak like features observed in most cases is an artifact of the change in phase angle of the output signal in the susceptibility measurements. The measured slope of the linear portion is -1.43 for the CdTe and $\leqslant 0.5$ for all the $Cd_{1-x}Mn_xTe$ films. This deviation is significant and is the same for all the measurements, thus not caused by the experimental errors. Clearly, the assumption that the d electrons are tightly localized is not valid. The crystalline bond ionicity of MnTe is 0.38 (Ref. 57) and that of CdTe is 0.72.[58] Considerable covalency in the case of MnTe and hence in $Cd_{1-x}Mn_xTe$ substantiates the possibility of delocalization of the d electrons and the d-d transitions do take place. These delocalized electrons contribute to the optical, electrical, and magnetic properties of $Cd_{1-x}Mn_xTe$ films. The CdTe films exhibit a slope of 1.43 in the absence of d-electron contributions from the MnTe sublattice and also due to high Cd-Te bond ionicity. Although the interpretation of the resistivity data has yielded an indirect information about the nature of spin glasses, a

more comprehensive theory may be required for the study of spin-glass dynamics. At standard magnetic transitions, the electrical resistivity has an energylike behavior.[59,60] The lack of any detectable singularity in the resistivity data of the spin glasses shows that they are first-order transitions.[60]

IV. CONCLUSIONS

Thin films of $Cd_{1-x}Mn_xTe$ in a wide Mn concentration range [dilute ($X<0.1$) as well as alloyed ($X>0.1$)] have been prepared by sublimation on Corning 7059 glass substrates. The dynamic susceptibility and electrical resistivity measurements have been performed in a 300–20-K temperature range. The films have been found to be paramagnetic at temperatures >100 K. While the films in the dilute range exhibit a behavior like that of the CdTe films, the higher Mn concentration ($X>0.25$) films exhibit a low-temperature phase which has been shown to be spin glass. The spin-glass transition temperatures and consequently the first-neighbor exchange interaction between the Mn ions have been found to be higher for the thin films than those reported for the single crystals. These have been shown to be a consequence of the interstitial MnTe sublattice formation in the high Mn concentration films. These Mn interstitial states have been shown to be nonlocalized in nature due to the high covalent nature of the Mn-Te bond.

ACKNOWLEDGMENTS

One of the authors (S.C.) would like to thank Dr. Kanwal Jeet Singh for many helpful discussions and P. D. Paulson for help in deposition of the thin films.

*Present address: Material Science Division, Indira Gandhi Center for Atomic Research, Kalpakkam 603 012, Tamil Nadu, India.

[1] J. K. Furdyna and J. Kossut, in *Diluted Magnetic Semiconductors*, edited by J. Furdyna and J. Kossut, Semiconductors and Semimetals Vol. 25 (Academic, San Diego, 1988).
[2] N. B. Brandt and V. V. Moshchalkov, Adv. Phys. **33**, 193 (1984).
[3] J. K. Furdyna, J. Appl. Phys. **53**, 7637 (1982).
[4] J. A. Gaj, J. Phys. Soc. Jpn. Suppl. A **49**, 797 (1980).
[5] R. R. Galazka, in *Semimagnetic Semiconductors based on Hg-MnTe and CdMnTe*, Proceedings of the 14th International Conference on the Physics of Semiconductors, edited by B. L. H. Wilson, IOP Conf. Proc. No. 43 (Institute of Physics and Physical Society, London, 1979), p. 133.
[6] R. R. Galazka, *Proceeding of the International Conference on Narrow Gap Semiconductors*, Lecture Notes in Physics Vol. 152 (Springer-Verlag, Berlin, 1982), p. 294 and references therein.
[7] S. B. Oseroff, Phys. Rev. **25**, 6584 (1982).
[8] T. Dolling, T. M. Holden, V. F. Sears, J. K. Furdyna, and W. Giriat, J. Appl. Phys. **53**, 7644 (1982).
[9] A. K. Ramdas, J. Appl. Phys. **53**, 7649 (1982), and references therein.
[10] J. A. Gaj, R. R. Galazka, and M. Nawrocki, Solid State Commun. **25**, 193 (1978).
[11] A. Mycielski and J. Mycielski, J. Phys. Soc. Jpn. **49**, 809 (1980).
[12] R. R. Galazka and J. Kossut, *Lecture Notes in Physics* (Springer-Verlag, Berlin, 1980), Vol. 132, p. 245.
[13] M. Nawrocki, R. Planel, G. Fishman, and R. R. Galazka, Phys. Rev. Lett. **46**, 735 (1981).
[14] T. Dietl and J. Spalek, Phys. Rev. B **28**, 1548 (1983).
[15] S. H. Wei and A. Zunger, Phys. Rev. B **35**, 2340 (1987).
[16] B. E. Larson, K. C. Hass, H. Ehrenreich, and A. E. Carlsson, Solid State Commun. **56**, 347 (1985).
[17] J. A. Gaj, in *Diluted Magnetic Semiconductors* (Ref. 1), p. 276.
[18] N. Samarth and J. K. Furdyna, Proc. IEEE **78**, 990 (1990).
[19] J. K. Furdyna, J. Appl. Phys. **64**, R29 (1988).
[20] A. Twardowski, P. Glod, W. J. M. DeJonge, and M. Demianiuk, Solid State Commun. **64**, 63 (1987).
[21] J. K. Furdyna and N. Samarth, J. Appl. Phys. **61**, 3526 (1987).
[22] J. Spalek, A. Lewicki, Z. Twardowski, J. K. Furdyna, R. R. Galazka, and Z. Obuszko, Phys. Rev. B **33**, 3407 (1986); W. J. M. de Jonge and H. J. M. Swagten, J. Magn. Magn. Mater. **100**, 322 (1991).
[23] A. Twardowski, H. J. M. Swagten, W. J. M. de Jonge, and M. Demianiuk, Phys. Rev. B **36**, 7013 (1987); P. W. Anderson, in *Solid State Physics: Advances in Research and Applications*, edited by F. Seitz and F. Turnbull (Academic, New York, 1963), Vol. 14.
[24] R. R. Galazka, S. Nagata, and P. H. Keesom, Phys. Rev. B **22**, 3344 (1980).
[25] R. R. Galazka, J. Magn. Magn. Mater. **140–144**, 13 (1995); H. Bednarski and J. Cisowski, J. Cryst. Growth **159**, 1018 (1996).
[26] N. Samarth and J. K. Furdyna, Phys. Rev. B **37**, 9227 (1988).
[27] J. Villian, Z. Phys. B **33**, 31 (1979).
[28] N. D. Mermin and H. Wagner, Phys. Rev. Lett. **17**, 1133 (1966); H. J. Schulz, T. A. L. Ziman, and D. Poilblanc, J. Phys. (France) I **6**, 675 (1996).
[29] S. Venugopal, L. A. Kolodziejski, R. L. Gunshor, and A. K. Ramdas, Appl. Phys. Lett. **45**, 974 (1981); K. Ando and H. Akinaga, J. Magn. Magn. Mater. **140–144**, 2029 (1995).
[30] S. Chandra, L. K. Malhotra, and A. C. Rastogi, Thin Solid Films **238**, 167 (1994); J. Appl. Phys. **78**, 5645 (1995).
[31] Susceptibility Instrumentation Manual No. SRD 204, Sumitomo Heavy Industries Ltd., Precision Products Group, Chiyoda-ku, Tokyo, Japan, 1993 (unpublished).
[32] J. R. Gabriel, D. F. Johnston, and M. D. J. Powell, Proc. R. Soc. London Ser. A **264**, 503 (1961). Vol. 204.
[33] K. Binder and A. P. Young, Rev. Mod. Phys. **58**, 801 (1986).
[34] A. F. J. Morgownik and J. A. Mydosh, Solid State Commun. **47**, 325 (1983).
[35] K. V. Rao, M. Fahnle, E. Fingeroa, O. Beckmann, and L. Hedman, Phys. Rev. B **27**, 3104 (1983).
[36] C. A. Mulder, M. A. J. van Duyneveldt, and J. A. Mydosh, Phys. Rev. B **23**, 1384 (1981); A. Bruno and J. P. Lascaray, *ibid*. **38**, 9168 (1988).
[37] G. Toulouse, Commun. Phys. **2**, 115 (1977).
[38] K. Ando, K. Takahashi, and T. Okuda, J. Magn. Magn. Mater. **104–107**, 993 (1992); T. M. Giebultowicz, P. Klosowski, N. Samarth, H. Luo, J. K. Furdyna, and J. J. Rhyne, Phys. Rev. B **48**, 12 187 (1993).
[39] L. Lundgren, P. Sevedlindh, P. Nordled, and O. Beckman, Phys. Rev. Lett. **51**, 911 (1983).
[40] J. Rajchenbach and N. Bontemps, J. Phys. (Paris) Lett. **44**, L799 (1983).
[41] C. Paulsen, J. Hamida, S. J. Williamson, and H. Maletta, J. Appl. Phys. **55**, 1652 (1984).
[42] P. J. Ford and J. A. Mydosh, Phys. Rev. B **14**, 2057 (1976).

[43] J. S. Schilling, P. J. Ford, U. Larsen, and J. A. Mydosh, in *Amorphous Magnetism II*, edited by R. A. Levy and S. Hasegawa (Plenum, New York, 1977).
[44] O. Laborde and P. Radhakrishna, J. Phys. F **3**, 1731 (1973).
[45] E. Shanthi A. Banerjee, V. Dutta, and K. L. Chopra, Thin Solid Films **71**, 237 (1980).
[46] J. Seiden, Can. Res. Acad. Sci. Ser. B **282**, 149 (1976).
[47] J. R. Christman, *Fundamentals of Solid State Physics* (Wiley, New York, 1988).
[48] Y. S. Touloukian, R. W. Powell, C. Y. Ho, and P. G. Klemens, *Thermal Conductivity of Non-Crystalline Solids* (Plenum, New York, 1970).
[49] F. J. Blatt, *Physics of Electronic Conduction in Solids* (McGraw-Hill, New York, 1968).
[50] E. Conwell, in *Transport: The Boltzmann Equation*, edited by T. S. Moss, Handbook of Semiconductors (North-Holland, Amsterdam, 1982), Vol. 1.
[51] P. G. Clemens, in *Solid State Physics: Advances in Research and Applications*, edited by F. Seitz and D. Turnbull (Academic, New York, 1958), Vol. 7.
[52] G. A. Slack, in *Solid State Physics: Advances in Research and Applications*, edited by H. Ehrenreich, F. Seitz, and D. Turnbull (Academic, New York, 1979), Vol. 34.
[53] J. M. Ziman, *Principles of Theory of Solids* (Cambridge University Press, Cambridge, London, 1972).
[54] K. Schröder, *Electronic, Magnetic and Thermal Properties of Solid Materials* (Marcel Dekker, New York, 1978).
[55] J. Sakurai, Y. Kubo, T. Kondo, J. Pierre, and E. F. Bertaut, J. Phys. Chem. Solids **34**, 1305 (1973).
[56] K. Sugihara, J. Phys. Chem. Solids **34**, 1727 (1973).
[57] V. N. Kamat Dalal and R. B. Prabhu, Physica B & C **112B**, 42 (1982).
[58] S. Perkowicz, L. S. Kim, and P. Becla, Solid State Commun. **77**, 471 (1991).
[59] M. E. Fischer and J. S. Langer, Phys. Rev. Lett. **20**, 665 (1968).
[60] K. Binder and J. Stauffer, Z. Phys. B **24**, 407 (1976).